



저작자표시-비영리-변경금지 2.0 대한민국

이용자는 아래의 조건을 따르는 경우에 한하여 자유롭게

- 이 저작물을 복제, 배포, 전송, 전시, 공연 및 방송할 수 있습니다.

다음과 같은 조건을 따라야 합니다:



저작자표시. 귀하는 원저작자를 표시하여야 합니다.



비영리. 귀하는 이 저작물을 영리 목적으로 이용할 수 없습니다.



변경금지. 귀하는 이 저작물을 개작, 변형 또는 가공할 수 없습니다.

- 귀하는, 이 저작물의 재이용이나 배포의 경우, 이 저작물에 적용된 이용허락조건을 명확하게 나타내어야 합니다.
- 저작권자로부터 별도의 허가를 받으면 이러한 조건들은 적용되지 않습니다.

저작권법에 따른 이용자의 권리는 위의 내용에 의하여 영향을 받지 않습니다.

이것은 [이용허락규약\(Legal Code\)](#)을 이해하기 쉽게 요약한 것입니다.

[Disclaimer](#)

Thesis for the Degree of Master of Engineering

Compatibility and hydrolytic behaviors of
isomer polylactide/poly(butylene succinate)
mixtures by Langmuir technique



by

Donghyeok Im

Department of Polymer Engineering

The Graduate School

Pukyong National University

February 2021

Compatibility and hydrolytic behaviors of
isomer polylactide/poly(butylene succinate)
mixtures by Langmuir technique

(랑뮤어 기술을 이용한 이성질체
폴리락타이드/폴리부틸렌석시네이트
혼합물의 상용성 및 가수분해거동)

Advisor : Prof. Won-Ki Lee

by

Donghyeok Im

A thesis submitted in partial fulfillment of the requirements
for the degree of

Master of Engineering

in Department of Polymer Engineering, The Graduate School,
Pukyong National University

February 2021

Compatibility and hydrolytic behaviors of isomer
polylactide/poly(butylene succinate) mixtures
by Langmuir technique

A dissertation
by
Donghyeok Im

Approved by:



M. H. Kim

(Chairman) Prof. Munho Kim



(Member) Prof. Youngho Eom



(Member) Prof. Won-Ki Lee

February 19, 2021

CONTENTS

Contents	i
List of Tables	iii
List of Figures	iv
Abstract	vi
Chapter 1. Introduction	1
Chapter 2. Theoretical background	3
2.1 Biodegradable polymers	3
2.2 Poly(lactide) (PLA)	7
2.2.1. Synthesis of PLA	9
2.2.2. Control of molecular weight PLA	11
2.2.3. Property of PLA	12
2.2.4. Stereochemical PLA	14
2.3 Poly(butylene succinate) (PBS)	15
2.3.1. Synthesis of PBS	16
2.3.2. Properties of PBS	18
2.4 Langmuir-Blodgett films	19
2.4.1. Formation and stability of monolayers	20
2.4.2. Surface Pressure/Area Isotherms	21
Chapter 3. Experimental section	22
3.1 Materials	22
3.2 Synthesis and analysis	23
3.3 Langmuir trough	25

Chapter 4. Results & discussion	26
4.1 Surface Pressure/Area Isotherms	26
4.1.1. <i>l</i> -PLA, <i>dl</i> -PLA, and PBS monolayers	26
4.1.2. Identification of the stability of the monolayers in water subphase	29
4.2 Thermal properties	31
4.3 Pressure–Area isotherms of mixtures	34
4.3.1. Different types of mixtures (Mix, Unmix)	34
4.3.2. Different behaviors of mixtures (Mix, Unmix)	35
4.3.3. Compatibility of <i>l</i> -PLA/PBS mixtures	37
4.3.4. Compatibility of <i>dl</i> -PLA/PBS mixtures	39
4.4 Hydrolytic degradations of monolayers	41
4.4.1. Schematic representation of hydrolysis monolayers by Langmuir system	41
4.4.2. Area ratio vs time for PLA/PBS mixtures	43
4.4.3. Hydrolytic kinetics of binary monolayers	47
4.4.4. AFM Image	50
 Chapter 5. Conclusion	 52
References	53
Acknowledgement	60

List of Schemes

Scheme 1. Routes of poly(lactic acid) (PLA) synthesis from lactic acid.

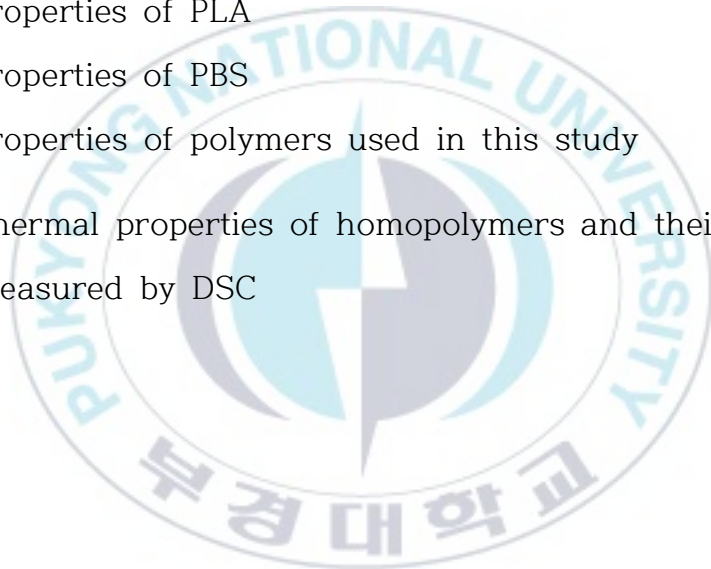
List of Tables

Table 1. Properties of PLA

Table 2. Properties of PBS

Table 3. Properties of polymers used in this study

Table 4. Thermal properties of homopolymers and their blends measured by DSC



List of Figures

Figure 1. Cyclic biological process of biodegradable polymers.

Figure 2. Representative biodegradable polymers based on two resources.

Figure 3. Schematic representation of PLA production

Figure 4. Synthetic tools for synthesis of PLA

Figure 5. Stereoisomeric forms of lactide

Figure 6. Synthetic routes of PBS (Up: Step I, Down: Step II)

Figure 7. Monolayer of polymer on a water surface.

Figure 8. Pressure-area isotherms of *l*-PLA, *dl*-PLA, PBS monolayers on subphase of pH 6.8 and their structures.

Figure 9. π -A isotherms of *l*-PLA (A) and PBS (B) at pH 6.8: a: measured at nearly 0 mN/m, b: re-measured after the compression to b', c: re-measured after the compression to c'.

Figure 10. DSC curves of *l*-PLA/PBS (A) and *dl*-PLA/PBS (B) blend films. The arrows indicate their T_g .

Figure 11. Pressure-area isotherms of Mix and Unmix *l*-PLA/PBS monolayers on subphases of pH 6.8: (A) 80/20, (B) 70/30, (C) 50/50, (D) 30/70, (E) 20/80. Dash lines are calculated by the additive rule.

Figure 12. Pressure-area isotherms of *dl*-PLA/PBS mixture monolayers on subphase of pH 6.8: (A) 80/20, (B) 50/50,

(C) 40/60. (D) 20/80. Dash lines were theoretically calculated by the additive rule.

Figure 13. Schematic representation of hydrolyzable polymeric monolayers on the water subphase.

Figure 14. Area ratio vs time for *l*-PLA/PBS (A) and *dl*-PLA/PBS (B) mixtures at 4 mN/m on subphase of pH 10.7. Dash lines (T) were calculated by the additive rule.

Figure 15. Area ratio vs time for *l*-PLA/PBS (Top) and *dl*-PLA/PBS (Bottom) mixture monolayers with different compositions at 4 mN/m on subphases of pH 10.7 : (A) 80/20, (B) 50/50, (C) 20/80 by mol%. Where a and b curves are from Unmix and Mix monolayers, respectively.

Figure 16. AFM images of *l*-PLA/PBS (A) and *dl*-PLA/PBS (B) mixture films with 20/80 by mol% before (left) and after (right) alkaline hydrolysis at pH 10.7 for 6 hr.

Langmuir 시스템을 이용한 이성질체 폴리락타이드/폴리부틸렌석시네이트 혼합물의 상용성 및 가수분해

임동혁

부경대학교 대학원 고분자공학과

요 약

Poly(lactide)s (PLAs) 및 Poly(butylene succinate) (PBS) 블렌드에 대한 다양한 연구들은 각기 상이한 결과를 나타내었다. 본 연구에서는 Langmuir 단분자막 장치를 이용하여 공기/물 계면에서 블렌드의 상용성과 가수분해 거동을 체계적으로 연구하였다. 비상용계 블렌드는 각각의 고분자 용액을 혼합하지 않고 각기 spreading한 단분자막을 모델로 하여 충분히 혼합한 블렌드 시스템과의 단분자막 거동을 비교, 분석하였다. 비상용계의 블렌드는 점유 면적 및 전이 영역에서 각 블렌드 성분의 특성을 나타내었으나, 충분히 혼합한 *l*-PLA/PBS 블렌드 단분자막의 점유 면적 및 전이 영역의 거동은 PBS 조성에 영향을 받았다.

l-PLA/PBS 블렌드의 상용성은 PBS 조성이 증가함에 따라 감소한 반면, *dl*-PLA/PBS 블렌드 단분자막은 전 조성에서 상용성을 나타냈다. 이러한 블렌드 단분자막의 상용성과 분해 특성을 연구하기 위해 일정한 표면 압력의 알칼리 수용액상(pH 10.7)에서 블렌드의 가수 분해 거동을 시간의 함수로 측정하였다. 상용성을 갖는 블렌드 단분자막은 각 고분자의 산술 평균보다 훨씬 느린 가수 분해 거동을 보였는데, 이러한 가수분해 지연은 PLA와 PBS 사슬 사이의 상호작용에 의한 결과로, 빠른 가수분해 특성을 가진 PBS 에스테르 결합에 대한 알칼리 이온의 공격을 지연시켜 주기 때문으로 판단된다. 이러한 결과는 생분해성 고분자의 초기분해속도를 제어하여 제품의 수명을 조절하는데 유용할 것이다.

CHAPTER 1. Introduction

Petroleum-based synthetic polymers have been widely acknowledged for their favorable properties and long-term stability. Many scientific and engineering efforts have been dedicated to the improvement of their properties and then low-density high performance polymers can replace conventional heavy materials such as ceramics and metals. Additionally, the use of polymeric disposable products is rapidly increasing due to their excellent physiochemical properties, low weight, transparency, low price, easy processability, etc. Therefore, the enormous amounts of waste plastics create serious environmental problems due to their long-term stability. To minimize these issues, there is increasing demand for the use of degradable and renewably derived polymers.

Polyesters are widely researched biodegradable polymers derived from renewable resources, and they include polylactide (PLA), poly(3-hydroxybutyrate) (PHB), poly(butylene adipate-co-terephthalate) (PBAT), and poly(butylene succinate) (PBS). These materials are degraded by the cleavage of ester bond linkages under acidic or basic conditions or with enzyme [1-5]. However, wide applications of biodegradable polymers are limited by their insufficient properties. To improve their properties, various physical and chemical modifications have been applied [6-8]. Among biodegradable polymers, PLA is widely used in the biomedical and disposable

material fields but its brittleness hinders its use in broad applications [9-15]. Since PBS is a biodegradable polymer with high ductility [15], there are numerous studies on the properties of PLA/PBS blends [9-21]. However, studies on PLA/PBS blends have reached different conclusions with respect to their incompatibility [14-16], partially compatibility [9-13], and compatibility [17]. Park et al. [12] calculated the Flory-Huggins interaction parameter of melt *l*-PLA/PBS blends and concluded that the negative parameter, -0.15, means that they are fully compatible. From the T_g change in *l*-PLA, the compatibility of the blend was confirmed when the PBS composition was lower than 20 wt% [9,10]. Defeng Wu [16] studied the *l*-PLA/PBS blend in terms of the morphological and rheological aspects and reported that the blend was incompatible. Recently, Cheng Lin et al. [17] reported that simulation models of *l*-PLA/PBS blends with different composition ratios show that the blends have good compatibility at all compositions.

On the other hand, the degradation rate of biodegradable polymers or their blends is one of the most important properties because the lifetime of commercialized goods with these blends is closely related to the initial degradation rate. General polymeric goods should not be degraded during use, but the degradation of waste should occur quickly. On the other hand, a constant degradation rate of biopolymers is required for drug delivery.

Our previous studies [23-27] showed that the Langmuir polyester

monolayers at a constant surface pressure lead to a reduction in the occupied area when hydrolysis occurs. The area reduction as a function of time is a hydrolytic kinetic process at the molecular level. Additionally, the Langmuir technique can be applied to determine the compatibility of the binary mixture by measuring the occupied areas of the components. In this study, Langmuir trough was used to investigate the hydrolytic kinetics and compatibility of enantiomeric PLA/PBS mixture monolayers at the air/water interface.



CHAPTER 2. Theoretical Background

2.1. Biodegradable polymers

Biodegradable polymers have a significant dominance over petroleum-based non-degradable polymers concerning degradation. These polymers relate to a polymer that is deteriorated by itself as specified by several environmental factors such as humidity, macro, and microorganisms, in-vivo or in-vitro temperature conditions, and it can be renewed into the land and enrich it by being composted with microorganisms. Most biodegradable polymers are intended to degrade as a result of enzymatic degradation or hydrolysis of polymer chains into natural by products such as gases (CO_2 , N_2), water, biomass, and inorganic salts. These polymers can be adapted from natural resources or comparatively attributed to renewable and synthesized resources and principally composed of ester, ether, and amide functional groups. Mostly, the synthesis route of these polymers goes through the condensation reactions, ring-opening polymerization, and metal catalysts [28-30].

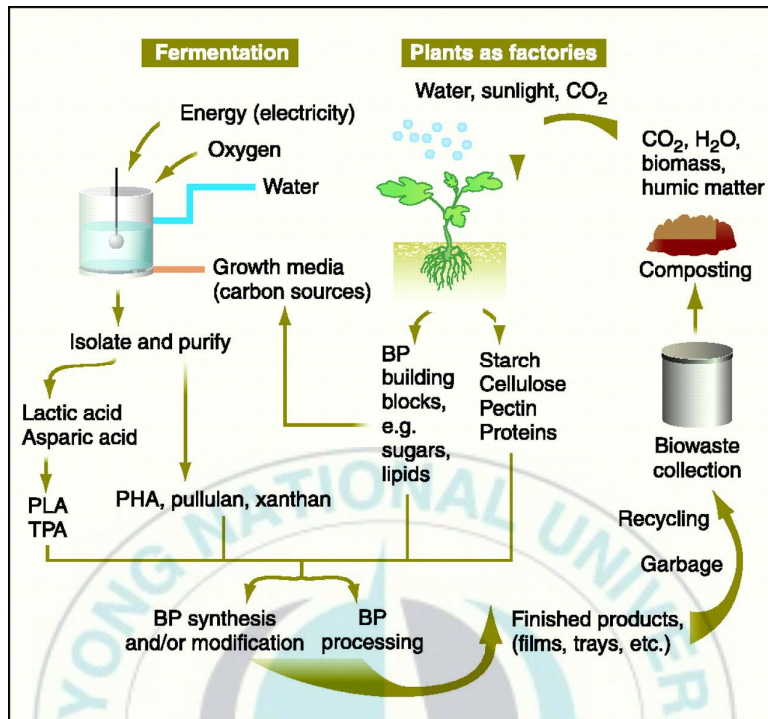


Figure 1. Cyclic biological process of biodegradable polymers [1].

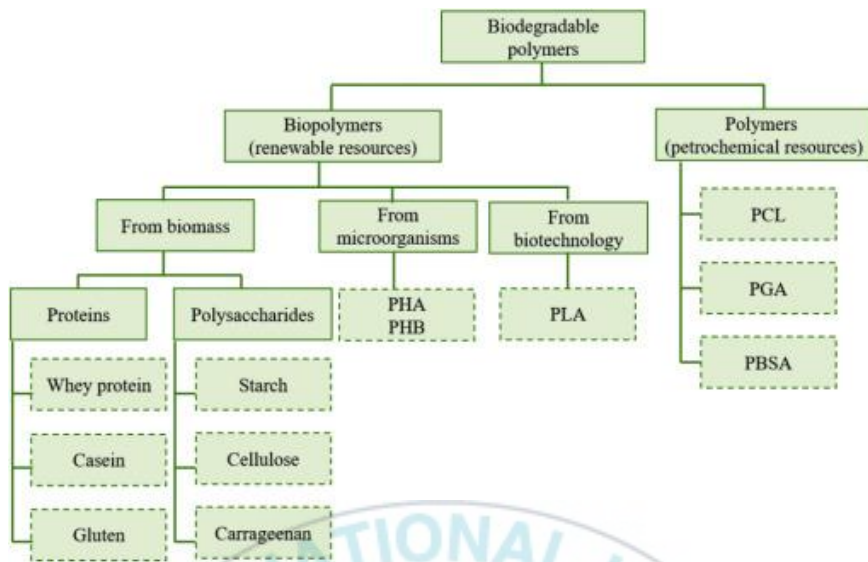
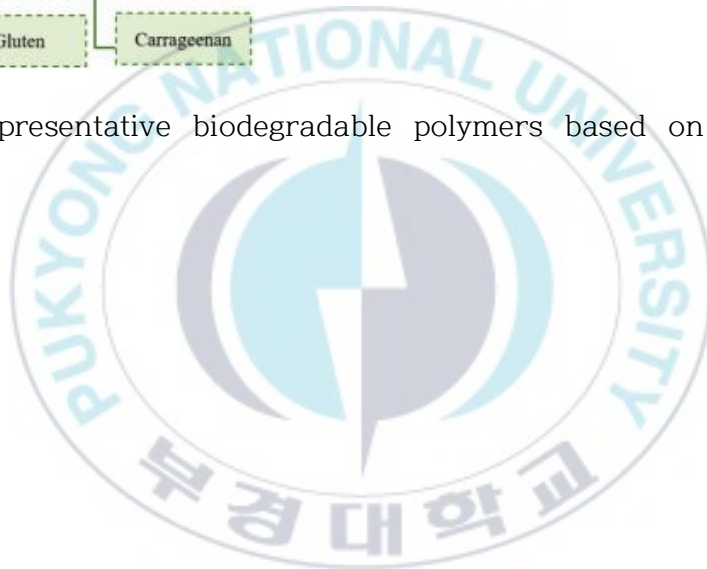


Figure 2. Representative biodegradable polymers based on two resources [31].



2.2. Poly(lacide) (PLA)

PLA is thermoplastics aliphatic polyester derived from renewable resources as an illustration of corn starch, sugarcane, tapioca roots, potato, or other fermented plant starch. It is a renewably-sourced, biodegradable, recyclable, and compostable polymer. PLA is one of the most promising eco-friendly biopolymer because it has better thermal processability compared to poly(γ -caprolactone) (PCL), poly(ethylene glycol) (PEG), and poly(hydroxyl alkanooate) (PHA). In the case of biodegradable polymers, degradation can be accelerated by transforming them into a form in which a functional group such as C=O bond is introduced into a typical synthetic polymer. In addition, since it has the advantage of being harmless to the human body, it is often used as a disposable product and medical applications [32-38].

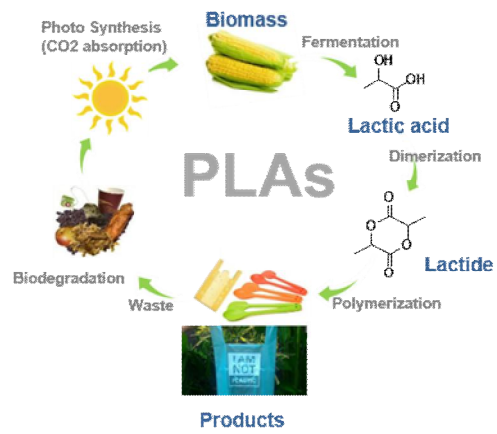
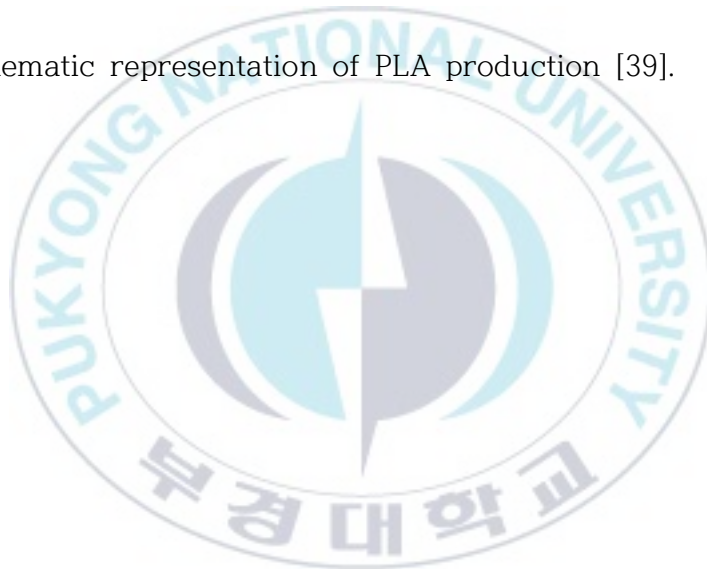


Figure 3. Schematic representation of PLA production [39].



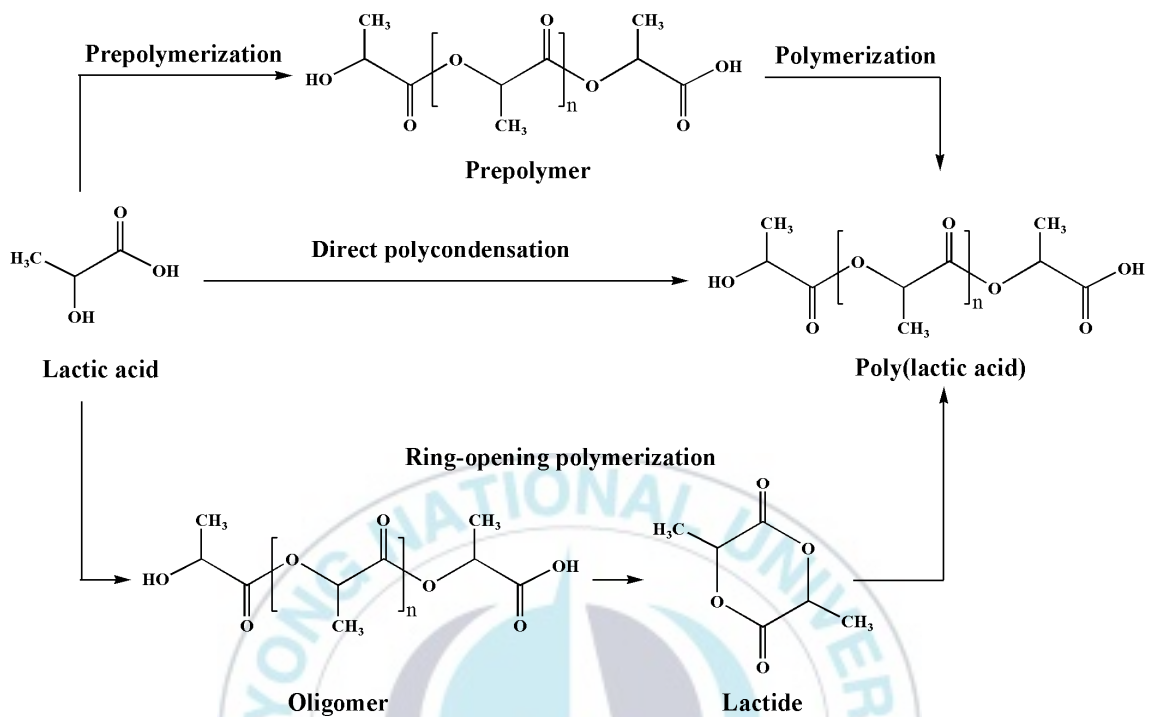
2.2.1 Synthesis of PLA

PLA can be synthesized by three major polymerization routes, which are schematically described below (Scheme 1).

1) Direct polycondensation reaction: Generally, the polycondensation of lactic acid is carried out in bulk by distillation of condensed water, with or without catalyst, while temperature and vacuum are gradually increased. It usually leads to low molecular weight polymers which then can be transformed into higher molecular weight polymers by the addition of chain coupling agents.

2) Ring-opening polymerization: PLA is synthesized by ring-opening polymerization whereby the end-points of polymer chains address lactide monomers to form the longer polymer chains using metal alkoxides as catalysts (Sn-based or Zn-based) resulting in high molecular weight PLA.

3) Azeotropic dehydrative condensation: PLA can be polymerized by direct polycondensation reaction through azeotropic dehydration, and it yields high molecular weight PLA by removing excess water during the polymerization reaction.



Scheme 1. Routes of poly(lactic acid) (PLA) synthesis from lactic acid.

2.2.2. Control of Molecular Weight of PLA

Usually, PLA can be synthesized by ring-opening polymerization. There are two different methods to synthesis PLA: 1) bulk polymerization, 2) solution polymerization. Generally, bulk polymerization is performed to obtain high molecular weight PLA, but it is very difficult to control the molecular weight. However, the molecular weight can be controlled by using the solution polymerization method by adjusting the catalyst concentration, reaction time, and temperature.

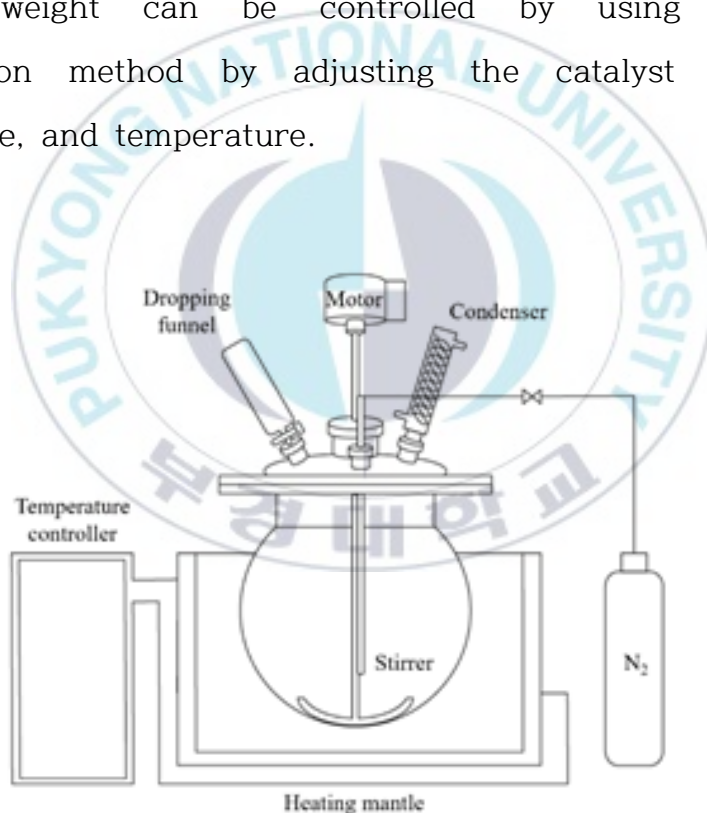
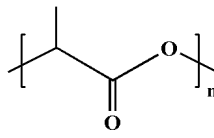


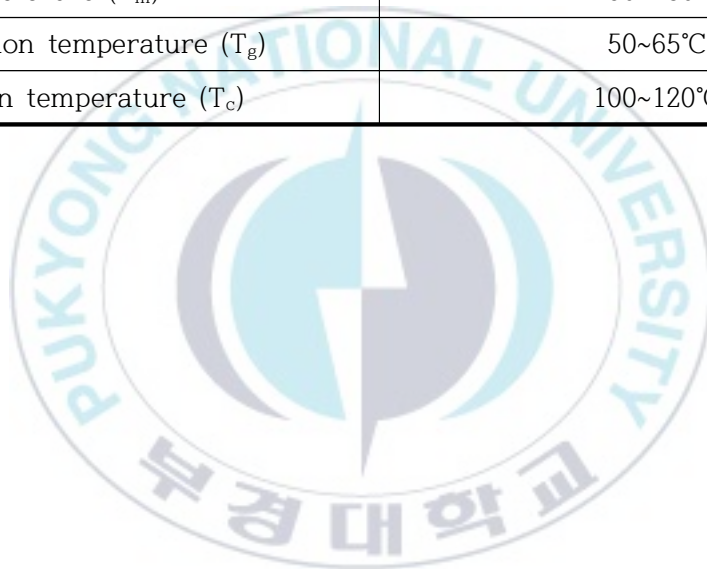
Figure 4. Synthetic tools for synthesis of PLA [40].

2.2.3. Property of PLA

PLA is a bio-based, biodegradable, and biocompatible polymer which has validated itself to be a favorable substitute for petroleum-based polymers. Most of the PLA are semi-crystalline polymers with 55 ~ 65 °C glass transition temperature and high melting point ca. 175 °C. It is widely commercialized in the food packaging industry and has been widely used not only in the areas of biomedical and pharmaceutical applications but also in the areas of protective clothing. Although PLA is brittle that it is not accordant with many manufacturing processes that relate to packaging. However, physical and chemical modifications, copolymerization, blending, alloying, or adding additives and fillers have been designed to improve efficiency and strengthened the properties.

Table 1. Properties of PLA

PLA	Properties
Structural formula	
Chemical formula	$(C_3H_4O_2)_n$
Density	1.210~1.430 g/cm ³
Melting temperature (T _m)	150~180°C
Glass transition temperature (T _g)	50~65°C
Crystallization temperature (T _c)	100~120°C



2.2.4. Stereochemical PLA

Lactide is a monomer having optical isomers of L, D, and meso type, and it is possible to synthesize PLA having various properties from amorphous to crystalline polymers through copolymerisation of l-lactide and d-lactide. Also, by forming a stereocomplex through blending between l-lactide and d-lactide, physical properties such as heat resistance, tensile strength can be improved, and the degradation rate can be retarded.

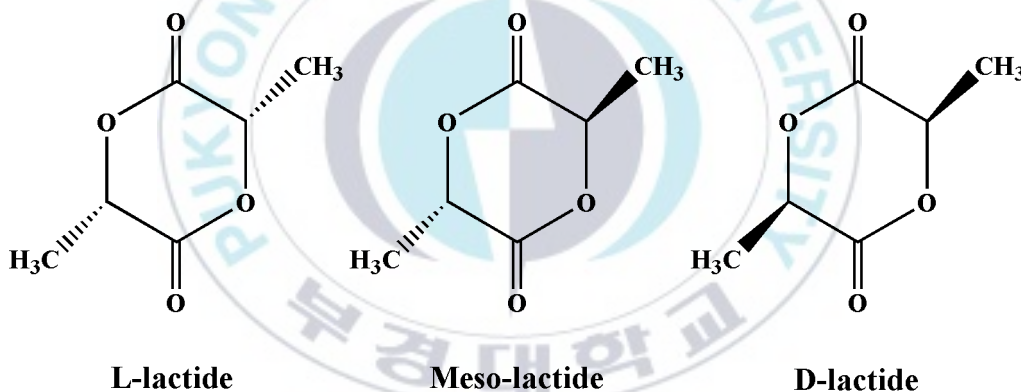


Figure 5. Stereoisomeric forms of lactide.

2.3 Poly(butylene succinate) (PBS)

PBS is classified among novel cost-efficient alternative to other biodegradable polymers such as PLA, PHB, and PBAT. It is having fair marketable quality with many stimulating features, including excellent melt processability, biodegradability, chemical, and thermal resistivity. Being a promising polymer for various potential applications because of its excellent processability, it is widely used in the textiles into mono- and multi-filaments, flat- and split-yarns, and also injection-molded commodities. Apart from that, PBS is used for food packaging, mulch films, plant plots, hygiene products, fishing nets, and fishing lines. Like polylactic acid (PLA), it fully degrades into biomass, CO₂, and H₂O and thus can be disposed of together with other organic waste.

2.3.1. Synthesis of PBS

PBS is largely manufactured by condensation polymerization of the succinic acid monomer and 1,4-butanediol. There are two main synthesis routes of PBS; the trans-esterification process (from succinate diesters) and the direct esterification process starting from the diacid. The direct esterification of succinic acid with 1,4-butanediol is the most prevalent way to manufacture PBS. It contains a two steps process; Step I. Excess of the diol is esterified with the diacid to form PBS oligomers with the elimination of H₂O. Step II. These oligomers are trans-esterified under vacuum to with the presence of titanium, zirconium, tin, or germanium derivatives catalyst to form a high molecular weight polymer [41].

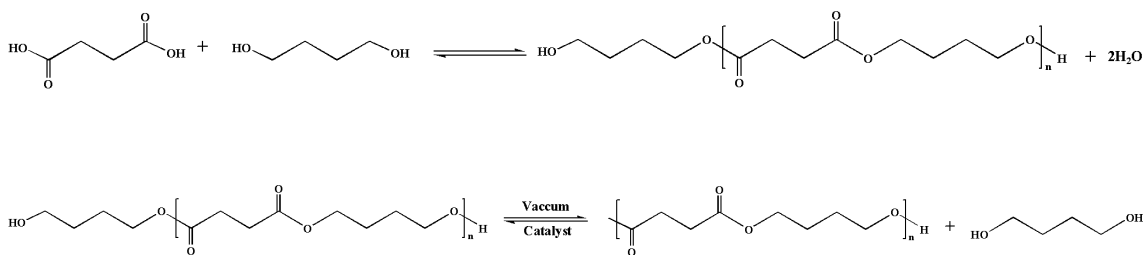


Figure 6. Synthetic routes of PBS (Up: Step I, Down: Step II)

Succinic acid (or dimethyl succinate) and 1,4-butanediol (BDO) are originated from sustainable and fossil-based feedstocks. Both are mainly obtained from maleic anhydride and can be produced either from sustainable feedstock as glucose and sucrose via fermentation or from petroleum-based feedstock.

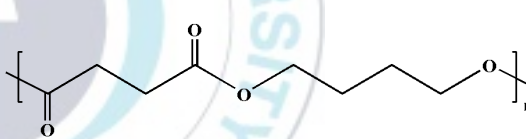
2.3.2. Properties of PBS

Poly(butylene succinate) (PBS) is a commercially available, aliphatic polyester with many interesting properties, including biodegradability, melt processability, and thermal and chemical resistance [42-44].

However, it is much more flexible and thus does not require plasticizers, but has a lower melting point than PLA (115°C ~ 160°C).

Glass transition temperatures (T_g) ranging from about -45°C to -10°C, and a density of about 1.25 g/cm³.

Table 2. Properties of PBS

PBS	Properties
Structural formula	 <chem>*C(=O)CCC(=O)OCCCCO*</chem>
Chemical formula	(C ₈ H ₁₂ O ₄) _n
Density	1.26 g/cm ³
Melting temperature (T_m)	90~100°C
Glass transition temperature (T_g)	-40~-25°C
Crystallization temperature (T_c)	100~120°C

2.4 Langmuir-Blodgett films

Langmuir film is a thin organic film one molecule thick. As a useful component in many practical and commercial applications such as sensors, detectors, displays, and electronic circuit components. The possibility to synthesize custom organic molecules and sophisticated thin film deposition techniques allows the creation of nanometer-scale electrical, optical and biologically active components.

The organic thin film can be deposited on a solid substrate by various techniques. The Langmuir-Blodgett (LB) technique is one of the most promising methods of preparing thin films.

- (A) Deliberate control of monolayer thickness
- (B) Uniform deposition of a monolayer
- (C) Possibility to create multi-layered structures with various layered structures

An additional advantage of Langmuir-Blodgett technology is the ability to deposit monolayers on almost any kind of solid substrate. In addition, it is possible to predict the degradation behavior and phase transition of polymers.

2.4.1. Formation and stability of monolayers

General monolayer-forming materials are amphiphilic in nature and possess two properties in the molecule: a hydrophilic (“water-friendly”) head-group, which is water-soluble, and an alkyl chain, which provides a hydrophobic (“water-unfriendly”) or oleophilic (oil-friendly) tail. When a polymer solution in an immiscible solvent for water such as chloroform is added in water, but then because of the immiscibility of chloroform with water, the chloroform spreads smoothly and covers all available areas. Likewise, the formation of monolayer depends on the immiscibility of the polymer solution in water. The evaporation of solvent from polymer solution results in the formation of a monolayer on the water surface that is because of the amphiphilicity of polymer molecules (as depicted in Figure 7). When the distance between polymer molecules is large, their interactions are small, and they can be regarded as forming a two-dimensional gas [22].



Figure 7. Monolayer of polymer on a water surface.

2.4.2. Surface Pressure/Area Isotherms

The single most significant indicator of the monolayer properties of a polymer is given by a plot of surface pressure as a function of the area of water surface available to each molecule. This is carried out at constant temperature and is accordingly known as a surface pressure/area isotherm, and is often abbreviated to “isotherm.” The equilibrium values can be determined on a point-to-point basis, but it is more important to register a pseudo-equilibrium isotherm by monitoring surface pressure while compressing the film at a constant rate. Depending on the material being investigated, repeated compressions and expansions may be necessary to realize a reproducible trace [22].

CHAPTER 3. Experimental section

3.1 Materials

L and D-lactide were procured from Purac (the Netherlands). PBS was supplied by SK Chemicals (Korea), and was purified by the dissolution/precipitation method using chloroform as the solvent and methanol as a non-solvent. Tin(II) 2-ethylhexanoate was purchased from Sigma-Aldrich (USA). Chloroform (99.8%) and methanol were obtained from Samchun (Korea). Sodium hydroxide was obtained from Icatayama Chemicals (Japan). All chemicals were used without further purification.



3.2 Synthesis and analysis

Synthesis of *l*-PLA and *dl*-PLA were carried out through the ring-opening polymerization of *l*-lactide and *d*-/*l*-lactide mixtures, respectively, in bulk at 145 °C for 6 h using tin(II) 2-ethylhexanoate (0.2 wt% of lactide) as a catalyst under vacuum. The acquired products were ultra-purified by the dissolution/precipitation method using chloroform and methanol as the solvent and non-solvent, respectively.

The weight average molecular weight (M_w) and polydispersity index (M_w/M_n) were evaluated by gel permeation chromatography (GPC, Shimadzu Corp.) in chloroform at a flow rate of 0.8 mL/min at 40 °C and polystyrenes (Shodex® STANDARD SM-105, Showa Denko K.K.) were used as standards. The investigations of thermal properties were carried out by differential scanning calorimetry (DSC 1, Mettler Toledo) at a of 10 °C/min heating rate under nitrogen atmosphere. The polymers used in this study are listed in Table 3. The surface morphological images were obtained by atomic force microscopy (AFM, SPA400, SII Nanotechnology Inc.) in tapping mode at a scan rate of 1 Hz. For the morphological investigation, 3 wt% polymer solutions were spin-coated on a glass substrate and used for AFM measurements.

Table 3. Properties of polymers used in this study

	M_w	PDI	T_g (°C)	T_m (°C)	Sources
<i>l</i> -PLA	580k	2.06	62.43	178.17	Synthesized for this study
<i>d,l</i> -PLA	54k	1.49	54.23	-	Synthesized for this study
PBS	48k	2.15	n.d.	113.83	Obtained from SK Chemical (Korea)



3.3. Langmuir trough

The Langmuir technique was applied to study the properties of polymeric binary monolayers, the surface pressure-area (π -A) and the hydrolytic behavior, by using a computer-controlled KSV-NIMA Langmuir probe system. One of the main advantages of the Langmuir monolayer technique is that it can control the lateral packing density in the monolayer, which is not achievable with any other conventional technique. Deionized water (DI, 18.2 M Ω ·cm) was obtained by an ultrapure water system (UNIONS, Sinhan Science). DI and chloroform were used as the subphase liquid and spreading solvent, respectively. *l*-PLA, *dl*-PLA, and PBS solutions were separately prepared by using a volumetric flask at a concentration of 1 μ mol/mL and mixture solutions (on a mol basis) were obtained by stirring the mixture of each homopolymer solution for 1 day. The Langmuir trough (580 x 145 x 4 mm³) was stabilized for an hour before use and filled with approximately 500 mL DI. After spreading the mixture (100 μ L for pressure-area (π -A) isotherm and kinetic measurements, unless otherwise stated), the solvent was allowed to evaporate over 1 min where the time was determined by the reproducibility of a the π -A curve. The compression rate of the barriers was 10 cm²/min throughout all experiments.

CHAPTER 4. Results & discussion

4.1. Surface pressure-area isotherms

4.1.1. *l*-PLA, *dl*-PLA, PBS monolayers

Most commercialized polymers are nondegradable, and large amounts of waste plastics cause environmental problems. To address this issue, many researchers have studied degradable polymers under natural conditions. However, their limited physical properties and high cost make it difficult to use these degradable polymers in a wide range of applications. Although a blend (or mixture) is an economical way to improve some weak physical characteristics, blend with desirable properties cannot be obtained without a favorable interaction between the blend components, namely, their miscibility or compatibility. The Langmuir technique has been used to identify well-defined monolayer behaviors of organic and polymeric materials that have achieved a hydrophobic/hydrophilic balance.

Despite extensive investigations on the compatibility of *l*-PLA/PBS blends, as mentioned above, the studies presented different conclusions in terms of the T_g behavior, interaction parameters, rheological properties, etc [9-17]. Previous studies [23-29] have shown that the Langmuir film balance has successfully been applied to investigate the compatibility and hydrolytic kinetics of polymer mixtures. Figure 8 represents the surface pressure-area (π -A)

isotherms for *l*-PLA, *dl*-PLA, and PBS monolayers on a subphase at pH 6.8. As shown in the previous studies [23,24], the π -A isotherm of *l*-PLA monolayers showed a transition of approximately 10 mN/m, and the *dl*-PLA monolayers collapsed at approximately 14 mN/m without a transition region. The surface pressure of *l*-PLA and *dl*-PLA monolayers sharply increased from above 2.5 mN/m, where the film state is changes from a gaseous state to an expanded state. However, the occupied area per monomer of PBS monolayers in the expanded state is much larger than that of the others. The repeating unit of PBS synthesized from succinic acid and 1,4-butanediol is composed of two ester groups (hydrophilic) and ethylene and butylene groups (hydrophobic) and then the monolayers in a gaseous π -A have large occupied areas due to the long-chain structure of the two separate hydrophilic and hydrophobic parts. When the monolayers are compressed, however, the long plateau region in the isotherm of PBS at approximately 5 mN/m is observed and the occupied areas before and after the plateau region are 45 and 10 Å²/repeating units, respectively.

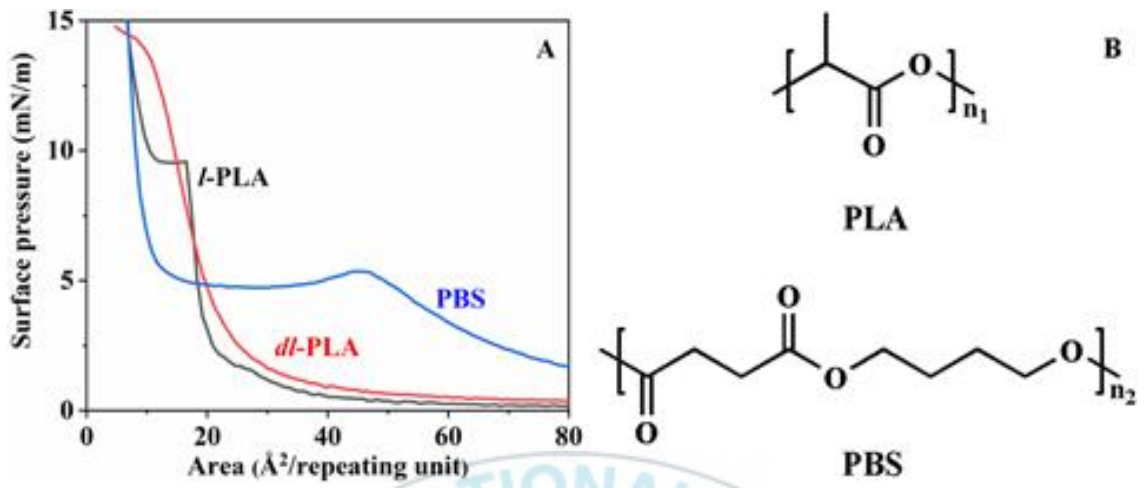


Figure 8. Pressure-area isotherms of *l*-PLA, *dl*-PLA, PBS monolayers on subphase of pH 6.8 and their structures.

4.1.2. Identification of the stability of the monolayers in water subphase

To study this plateau region, π -A isotherms of PBS and *l*-PLA monolayers were remeasured after compression to a certain area (the b` or c` point in Fig. 9A) and then after the compression is released to 0 mN/m, as shown in Figure 9, where the compression and release rates were the same at 10 cm²/min. Since the plateau region of the *l*-PLA film on DI has been interpreted as a phase transition [23], the recompressed π -A isotherm of *l*-PLA after compression to over 12 mN/m of the plateau region was close to the original isotherm. This indicates that the phase transition of *l*-PLA monolayers is reversible due to a weak transitional force. However, the recompressed π -A isotherm of PBS after compression to the middle in the plateau region (b` point in Fig. 9B) showed that the plateau region started at the first compressed point. Additionally, the plateau region was not observed in the recompressed π -A isotherm (c curve) after compression to over 12 mN/m (c` point). These conformational memory effects of PBS monolayers are due to their strong conformational stability. Once the conformational change at the air/water interface occurs, it does not recover when the compression is released.

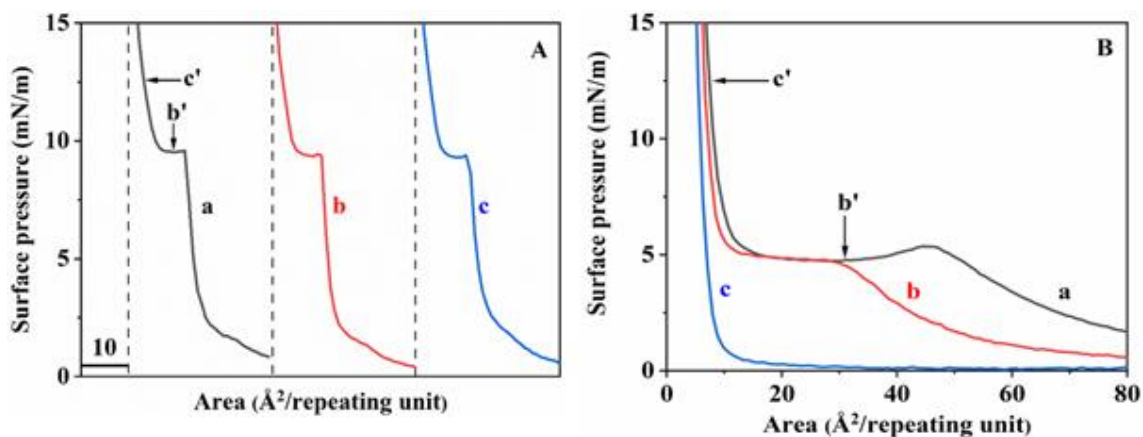


Figure 9. π -A isotherms of *l*-PLA (A) and PBS (B) at pH 6.8: a: measured at nearly 0 mN/m, b: re-measured after the compression to b', c: re-measured after the compression to c'.

Considering the differences in the structures of the repeating units of PLA and PBS, a notable parameter is the occupied area of each monolayer at a high surface pressure of over 10 mN/m, which follows the order of *dl*-PLA > *l*-PLA \geq PBS. Amorphous *dl*-PLA and semicrystalline *l*-PLA are configurational isomers, and the differences in the occupied areas are noticeable. However, the smaller occupied area of PBS at a high surface pressure, which has much longer backbone structure than that of PLA, can be explained by its chain folding structure at the air/water interface. Therefore, the long transition of PBS monolayers can be explained by chain folding.

4.2. Thermal properties

The thermal properties, T_g and T_m , of blends can be used to study their compatibility because in an incompatible blend system, the bulk property of each component in the blend is observable. It was reported that the T_g of the *l*-PLA/PBS blend by DSC measurements did not change much with the blend compositions and the blend was partially compatible [9,12]. Since the compatibility of a polymeric blend is strongly related to the interactions between the amorphous regions of each component, stereochemical PLAs, semicrystalline *l*-PLA and amorphous *dl*-PLA were used due to the compatibility and degradation behavior of the PLA/PBS blends. Figures 10A and 10B show the DSC thermograms of *l*-PLA/PBS and *dl*-PLA/PBS blends, respectively, after melt quenching at 200 °C. In the *l*-PLA/PBS blend, the T_c values of both polymers partly overlapped, and the T_m values of PBS were in similar temperature ranges. Therefore, the thermal behaviors of the *l*-PLA/PBS blend were analyzed in terms of the T_g of *l*-PLA. As shown in Table 4, the T_g values of the blends decreased with increasing the PBS composition, even though the T_g of the *l*-PLA/PBS blend at 20/80 wt% could not be determined due to the resolution limit of DSC or due to the compatibility. The T_g depression of the *l*-PLA/PBS blend is much smaller than those calculated by the Fox equation, as reported by others [9,12].

A similar thermal behavior was observed in the *dl*-PLA/PBS blend. However, the depression of the T_g of the blends greatly increased; with an 80/20 composition, the T_g values of the *l*-PLA/PBS and *dl*-PLA/PBS blends were approximately 59 °C and 46 °C, respectively, whereas the T_g values of *l*-PLA and *dl*-PLA were approximately 62 °C and 54 °C, respectively. With over 20 wt% of PBS in the blend, the T_g of the blends slightly decreased. These results support that the interaction between PLA and PBS preferentially occurs in amorphous regions.

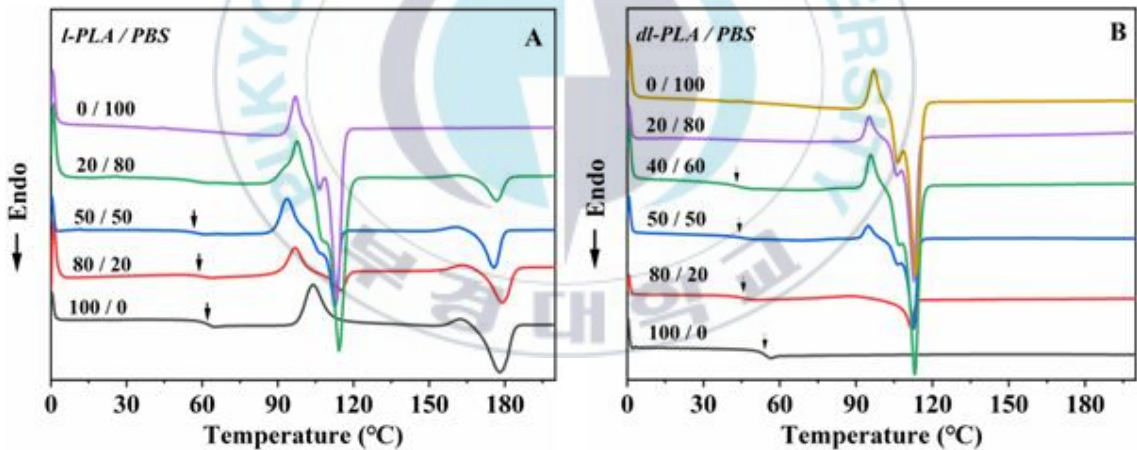


Figure 10. DSC curves of *l*-PLA/PBS (A) and *dl*-PLA/PBS (B) blend films. The arrows indicate their T_g .

Table 4. Thermal properties of homopolymers and their blends measured by DSC

Sample (by wt%)	T _g (°C)	T _{m1} (°C)/ΔH _i (J/g)	T _{m2} (°C)
<i>l</i> -PLA	62.43	178.17 / 34.54	-
<i>dl</i> -PLA	54.23	-	-
PBS	-	-	113.83
<i>l</i> -PLA/PBS (80/20)	58.72	179.17 / 25.1	115
<i>l</i> -PLA/PBS (50/50)	56.86	175.83 / 19.01	112.83
<i>l</i> -PLA/PBS (20/80)	-	176.83 / 8.35	114.67
<i>dl</i> -PLA/PBS (80/20)	45.9	-	111.83
<i>dl</i> -PLA/PBS (50/50)	43.1	-	112.83
<i>dl</i> -PLA/PBS (40/60)	42.97	-	113.67
<i>dl</i> -PLA/PBS (20/80)	-	-	113



4.3. Pressure-area isotherms of mixtures

4.3.1. Different types of mixtures (Mix, Unmix)

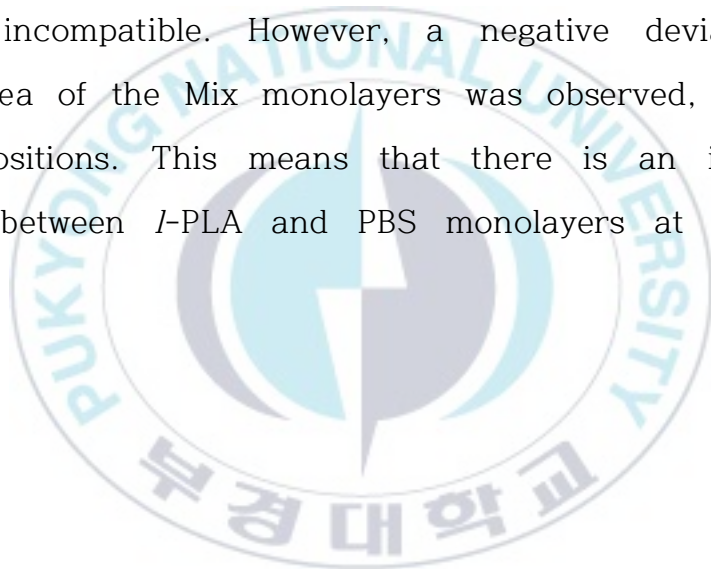
The compatibility of binary polymeric monolayers at the air/water interface has been studied by two methods: by a change in the transition and by plotting the mean area at a constant surface pressure [30-32]. The mixed monolayers with a linear relationship were regarded as an ideal mixture or as a completely incompatible mixture. Kawaguchi and Nishida reported that a negative deviation means that the binary mixture is considered to be stable and compatible whereas a positive deviation indicates that the mixture is less stable than the components alone at the interface [30,32].

To understand the π -A behaviors of *l*-PLA/PBS binary monolayers in terms of their compatibility, different types of mixture monolayers were prepared: one type consists of well-mixed (Mix) monolayers by spreading of the mixture solution after vigorous stirring for 3 days, and the other type consists of unmixed (Unmix) monolayers prepared by separately spreading each component solution on the subphase. The sample codes, Mix-L80 and Mix-DL80, indicate *l*-PLA/PBS and *dl*-PLA/PBS mixtures with an 80/20 composition by mol%, respectively.

4.3.2. Different behaviors of mixtures (Mix, Unmix)

Figure 11 shows the π -A curves of Mix and Unmix monolayers on the subphase at pH 6.8. The separated regions of the spreading of each polymer solution (Unmix) results in a sea-island morphology and then the monolayers are in completely incompatible state. As expected, the Unmix monolayers showed two transition regions at approximately 5 and 10 mN/m which correspond to the transitions of PBS and *l*-PLA monolayers, respectively, regardless of the mixture composition. However, the π -A curves of the Mix monolayers showed quite different behaviors from those of the Unmix monolayers. Below 40 mol% *l*-PLA, the transition was not detected because its transition region was too short or it disappeared, but all Unmix monolayers showed a clear transition of PBS. The PBS transition in the π -A curve of Mix monolayers systematically changed with the change in composition. The π -A curve of Mix-L80 did not show the PBS transition, the transition of Mix-L70 monolayers occurred in the surface pressure range from 6 to 8 mN/m over a narrow area range, and the Mix-L20 monolayers showed a flat region approximately 5.5 mN/m. Therefore, the conformational changes in the PBS monolayers in the mixture were disturbed due to the homogeneous distribution of each chain.

As mentioned above, the compatibility of mixture monolayers has often been studied by the change in the occupied area of mixture monolayers. The dotted lines in Figure 11 correspond to the mean area as a function of surface pressure. Below the surface pressure of the PBS transition, the areas occupied by the Unmix monolayers were very similar to those calculated by the additive rule. This finding is supported by the fact that the Unmix monolayers are completely incompatible. However, a negative deviation in the occupied area of the Mix monolayers was observed, regardless of their compositions. This means that there is an intermolecular interaction between *l*-PLA and PBS monolayers at the air/water interface.



4.3.3. Compatibility of *l*-PLA/PBS mixtures

All π -A curves of the Unmix monolayers showed a PBS transition at approximately 5 mN/m, which is similar to the surface pressure of the PBS transition itself. However, the *l*-PLA transition was observed in the Unmix monolayers with a *l*-PLA composition 50 mol% due to the sensitivity limit from its short transition region. The transition region in the π -A curve of Mix monolayers would be affected by their mixing morphology. Mix-L80 did not show the PBS transition whereas the *l*-PLA transition was clearly observed at the same surface pressure as Unmix-L80. As the PBS content in the mixture was increased to 50 mol%, namely, Mix-L70 and Mix-L50, the transitions occurred over wide surface pressure ranges, 6-8 mN/m, which are higher than those of neat PBS. The sloped, not plateaued, PBS transitions indicate that the transition is delayed by other adjacent chains. However, over 50 mol% PBS, namely, Mix-L30 and Mix-L20, the transitions of mixtures are very similar to that of neat PBS. Above the surface pressure of the PBS transition, the occupied areas of the Mix monolayers were larger than those of the Unmix or theoretical monolayers. This is clear if we consider that the conformational change in PBS monolayers in the mixture is disturbed by the neighboring PLA chains. Therefore, *l*-PLA/PBS mixture monolayers have partial compatibility which increases with the *l*-PLA composition.

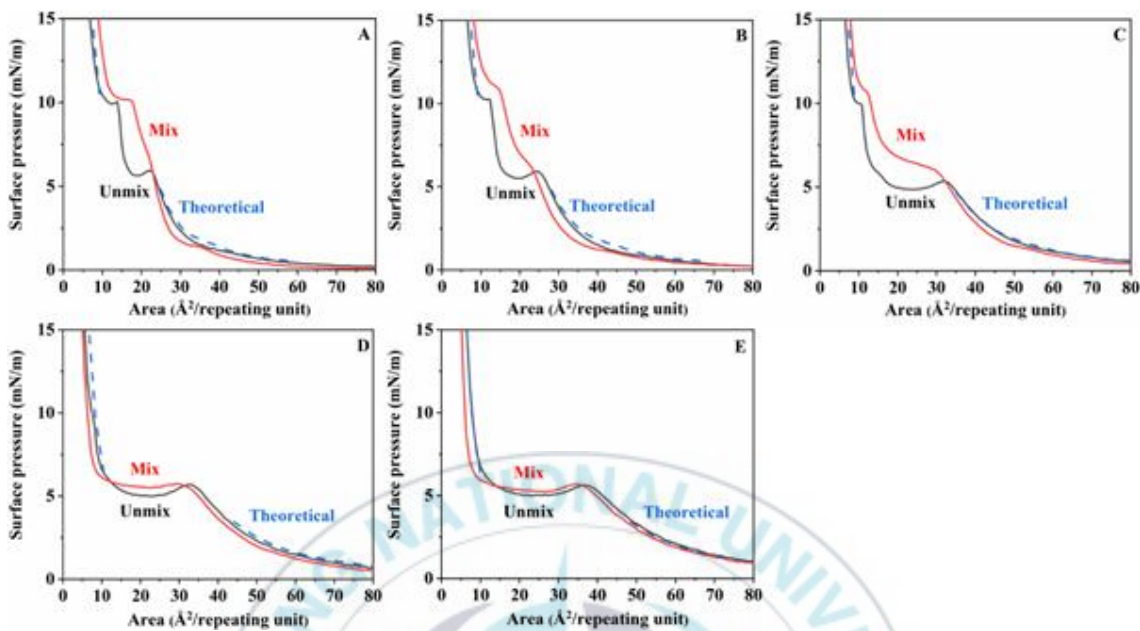


Figure 11. Pressure-area isotherms of Mix and Unmix *l*-PLA/PBS monolayers on subphases of pH 6.8: (A) 80/20, (B) 70/30, (C) 50/50, (D) 30/70, (E) 20/80. Dash lines are calculated by the additive rule.

4.3.4. Compatibility of *dl*-PLA/PBS mixtures

Since molecular interactions between polymer chains preferentially occur in the amorphous region, amorphous *dl*-PLA was used in the mixture instead of semicrystalline *l*-PLA. Figure 12 represents the π -A curves of Mix and Unmix *dl*-PLA/PBS monolayers with different compositions. Similar to those of the *l*-PLA/PBS mixture system, the π -A isotherms of the Unmix monolayers showed a clear phase transition of PBS at approximately 5 mN/m, regardless of composition. Additionally, the occupied area range of the transition region linearly increased with the PBS composition. However, the Mix monolayers showed different π -A behaviors. Mix-DL80 did not show any plateau or transition region, and the occupied area continuously increased with surface pressure over 12 mN/m. In the π -A isotherm of Mix-DL50, a short inflection behavior near 8 mN/m was observed. Above 50 mol% PBS in the mixture, the π -A isotherms showed plateau regions at approximately 8.5 mN/m, which was much higher than the surface pressure of neat PBS monolayers (5 mN/m). Additionally, the occupied area range of the transition region decreased to approximately 50%. Therefore, homogeneous mixing with *dl*-PLA substantially stabilized the PBS monolayers, and then the PBS transition occurred at a higher surface pressure. As mentioned, in the *l*-PLA/PBS mixture monolayers, these behaviors might indicate

that the PBS transition would be disturbed by homogeneously mixed *dl*-PLA chains in the mixture. Below 5 mN/m, the π -A curves of the Unmix monolayers almost overlapped with those theoretically calculated by the additive rule, but the π -A curves of the Mix monolayers showed a negative deviation, regardless of composition. These results might indicate that the *dl*-PLA/PBS mixture monolayers are compatible.

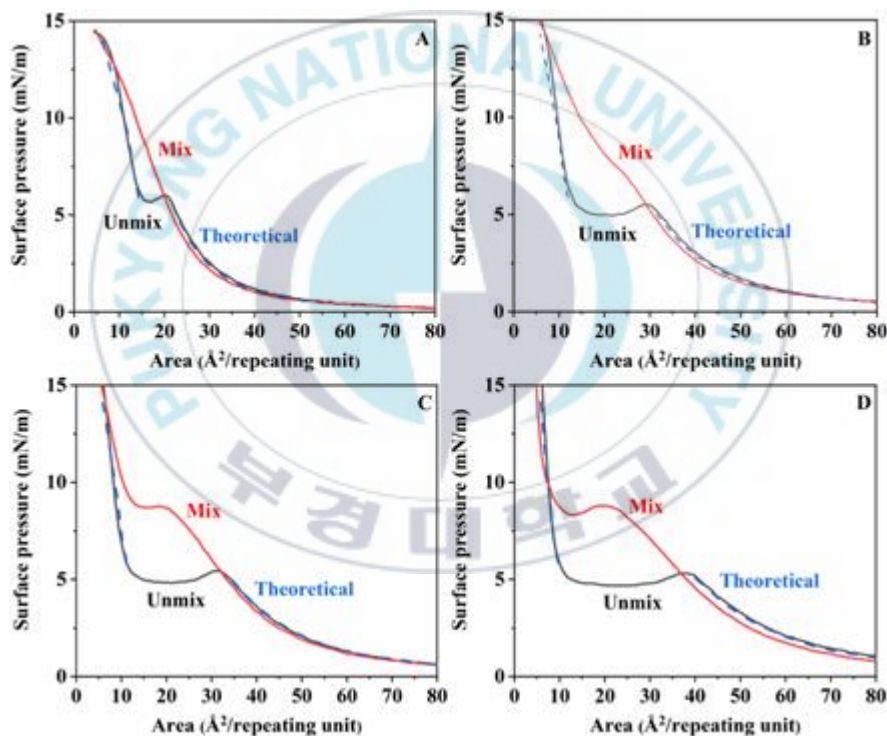


Figure 12. Pressure-area isotherms of *dl*-PLA/PBS mixture monolayers on subphase of pH 6.8: (A) 80/20, (B) 50/50, (C) 40/60. (D) 20/80. Dash lines were theoretically calculated by the additive rule.

4.4. Hydrolytic degradations of monolayers

4.4.1. Schematic representation of hydrolysis monolayers by Langmuir system

The degradability of biomaterials is one of the most important properties because of the lifetime of commercialized products. The Langmuir technique is a very useful tool to measure the hydrolytic kinetics of hydrolyzable polyesters at the molecular level [23-26]. This method provides a quantitative analysis of the in situ enzymatic or hydrolyzable degradation rate of polyester monolayers. The rate of their hydrolytic degradation is primarily affected by the accessibility of subphase ions to the ester bonds of monolayers and the bond strength, resulting in water-soluble oligomers. As hydrolyzed low molecular weight particles dissolve into the subphase, the occupied area at a constant surface pressure decreases. Therefore, the $1-A/A_0$ value with hydrolysis time is the degradation rate, where A and A_0 are the occupied areas after degradation time, t , and 0 , respectively.

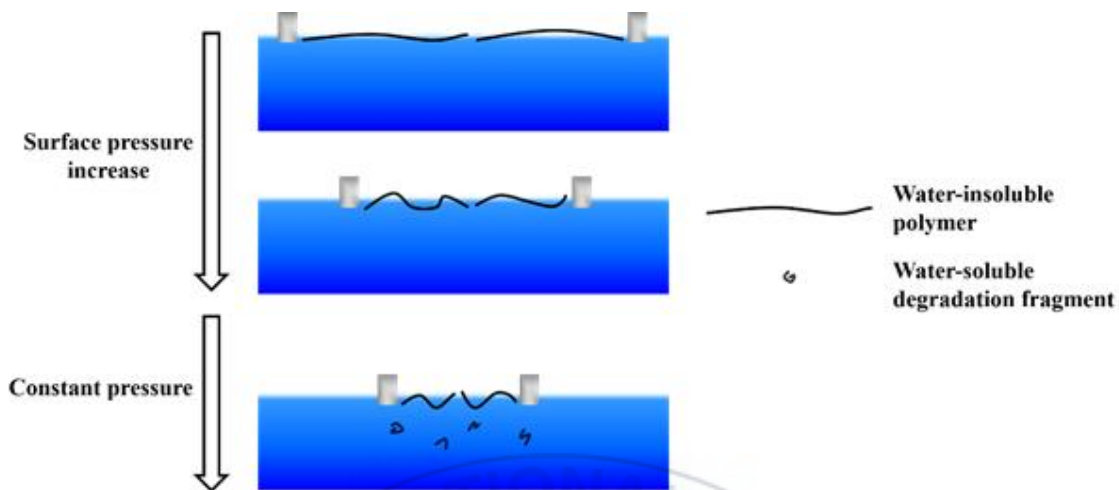
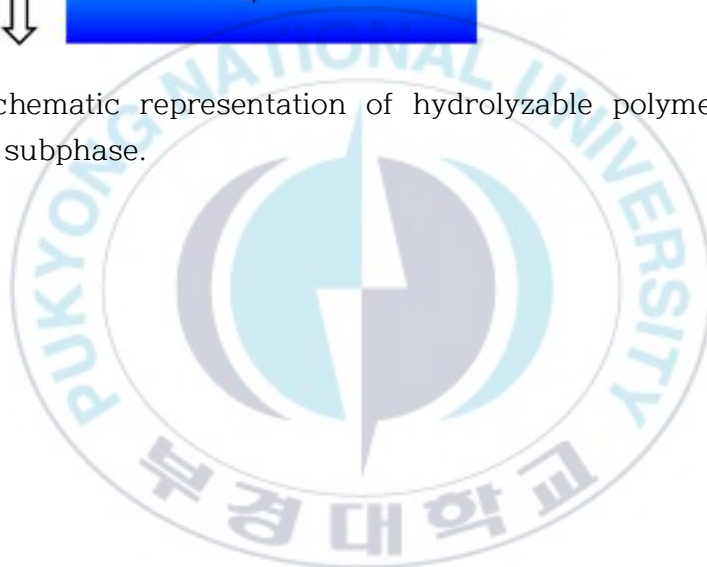


Figure 13. Schematic representation of hydrolyzable polymeric monolayers on the water subphase.



4.4.2. Area ratio vs time for PLA/PBS mixtures

All alkaline degradation experiments of monolayers were conducted at pH 10.7, which was controlled by adding NaOH solution. A constant pressure of 4 mN/m was used because the occupied area of the mixture monolayers is sensitive around the PBS transition of approximately 5 mN/m. A value of $t = 0$ is considered when the surface pressure becomes the desired value. To investigate any hydrolysis that occurs during compression, the π -A isotherm of the Unmix-L50 monolayer was measured with pause times of 0 and 60 min before compression. The results showed that there is little difference in the occupied area (not shown here). Figure 14 shows the change in areas (A/A_0) occupied by *l*-PLA, PBS, *dl*-PLA, and their mixtures with different compositions with exposure time on the subphase at pH 10.7 with a constant surface pressure of 4 mN/m. Under these measurement conditions, the occupied areas of PBS monolayers decreased to 30% ($A/A_0 = 0.3$) of the initial area after approximately 11 min of exposure time, while the *l*-PLA monolayers remained at approximately 88% ($A/A_0 = 0.88$) after 1 h. Although the M_w of *l*-PLA is much higher than that of PBS, a similar behavior was observed in the alkaline hydrolysis of *dl*-PLA monolayers with $M_w = 46k$. The faster alkaline hydrolysis of PBS monolayers can be explained by two factors: a larger occupied area per repeating unit

and the greater hydrophilicity of PBS. At a constant surface pressure of 4 mN/m, the occupied areas of *l*-PLA, *dl*-PLA, and PBS monolayers at pH 10.7 were 21, 28, and 54 Å²/repeating unit, respectively. The larger the occupied area is, the more alkaline ions there are under the monolayers. The contact angles of *l*-PLA and PBS to water were 72° and 64°, respectively. The stronger the hydrophilicity of the monolayer is, the more submerged the monolayer is into the subphase. Therefore, the PBS monolayers showed much faster alkaline hydrolysis than *l*-PLA and *dl*-PLA.

Since the two mixture monolayers *l*-PLA/PBS and *dl*-PLA/PBS at pH 6.8 showed different behaviors in the π -A isotherm curves, the hydrolytic behavior of the mixture monolayers on the alkaline subphase at pH 10.7 is related to their morphology or compatibility. In Figures 14A and 14B, experimental and theoretical kinetic curves of both mixture monolayers are shown when the monolayers are maintained at 4 mN/m on the subphase at pH 10.7. The theoretical curves (T_{MIX}) were calculated by the following equation:

$$T_{\text{MIX}} = M_{\text{PLA}} \cdot A_{\text{PLA}} + M_{\text{PBS}} \cdot A_{\text{PBS}}$$

where M and A represent the mole fraction in the mixture and the experimental occupied area at a particular surface pressure, respectively.

The degradation rate of the mixture monolayers decreased with increasing PLA composition due to the fast degradation of PBS. Although the degradation behavior of *dl*-PLA is not significantly different from that of *l*-PLA, both mixture monolayers showed different kinetic behaviors. The hydrolytic rate of the incompatible *l*-PLA/PBS mixture with 20/80 mol% is slightly higher than the theoretical rate, whereas the hydrolytic rates of the other mixtures are much slower than their theoretical values.

The fast hydrolytic rate of incompatible *l*-PLA/PBS can be explained by the dilution effect [24], in which there is preferential attack of PBS chains and increasing alkaline ions per PBS unit area. In the compatible *dl*-PLA/PBS mixture, however, all kinetic rates of mixtures were much lower than their theoretical rates. These large deviations between experimental and theoretical data can be explained by the fact that the hydrolysis of PBS chains is disturbed by adjacent PLA chains. In other words, morphological changes or changes in the surrounding conditions of PBS chains by homogeneous mixing with PLA chains determine their hydrolytic stability.

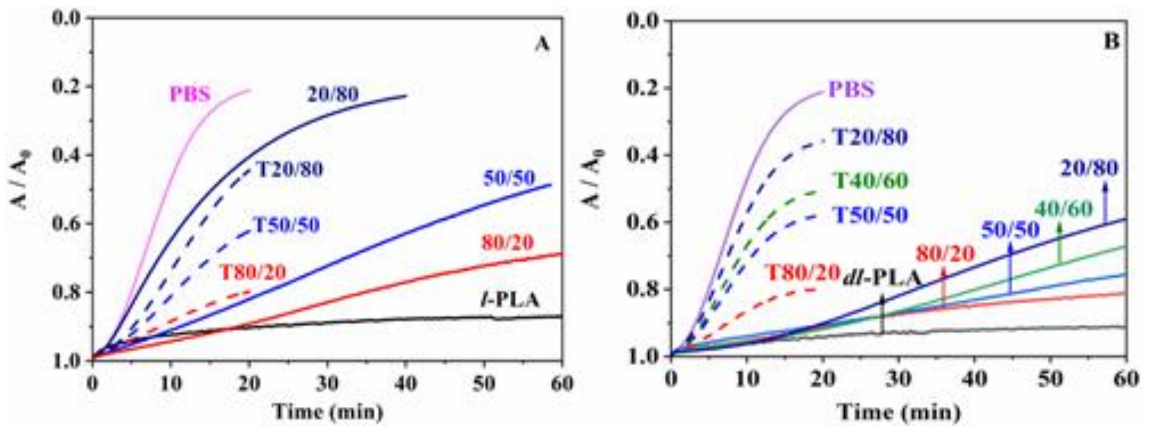
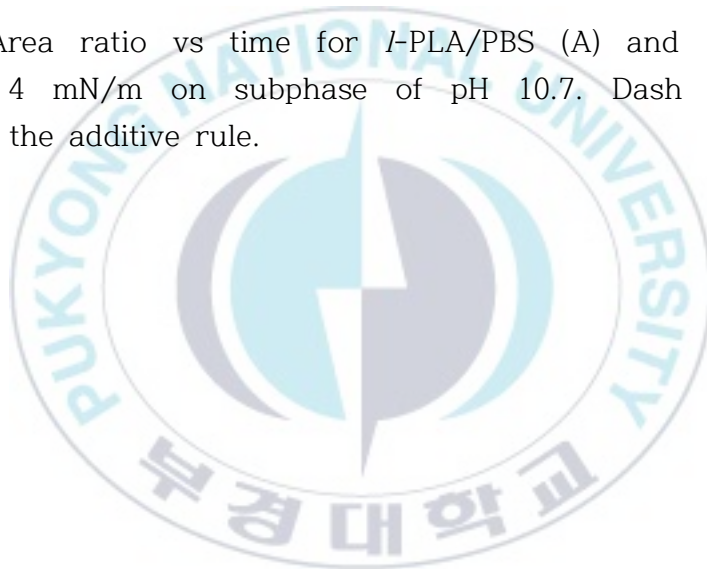
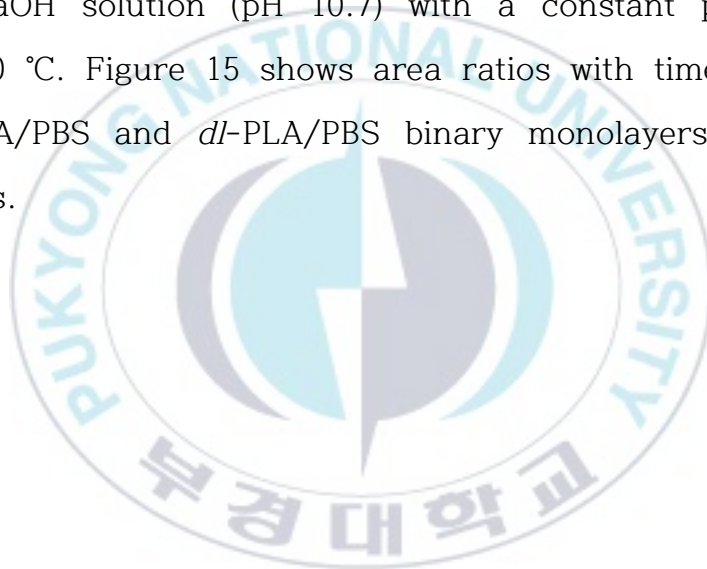


Figure 14. Area ratio vs time for *l*-PLA/PBS (A) and *dl*-PLA/PBS (B) mixtures at 4 mN/m on subphase of pH 10.7. Dash lines (T) were calculated by the additive rule.



4.4.3. Hydrolytic kinetics of binary monolayers

To further understand the hydrolytic behaviors of both mixture monolayers on alkaline subphases, experiments were performed to study the hydrolytic kinetics of unmixed binary monolayers by separately spreading each component solution as an incompatible model system, as mentioned before. The experiments were carried out with NaOH solution (pH 10.7) with a constant pressure of 4 mN/m at 20 °C. Figure 15 shows area ratios with time for Mix and Unmix *l*-PLA/PBS and *dl*-PLA/PBS binary monolayers with various compositions.



l-PLA/PBS monolayers showed faster hydrolysis than *dl*-PLA/PBS monolayers, regardless of the mixing state. Additionally, the hydrolytic rate of the Unmix monolayers (a in Figure 15) is much faster than that of the Mix monolayers, except for *l*-PLA/PBS 20/80 mol%, which showed little difference in the rate. Therefore, the hydrolytic kinetics of mixtures can affect their morphology. Additionally, the hydrolytic processes of both Unmix monolayers occur via two-step kinetics. Steps 1 and 2 were divided by the extrapolated onset, which denotes the remaining area ratio at which Step 2 begins. The A/A_0 at the initial stage rapidly decreased (Step 1) and then became slow (Step 2). The hydrolytic behavior in Step 1 is attributed to the preferential hydrolysis of PBS chains in the sea-island morphology. During Step 1, the dissolved fragments resulted in hydrolysis, the remaining monolayer chains were rearranged, and the interface (interaction) between PLA and PBS chains increased. Therefore, the hydrolytic kinetics in Step 2 are similar to those of the Mix systems. A noticeable point is the A/A_0 at which Step 2 starts. Although the kinetic slopes of the Unmix *l*-PLA/PBS in Step 1 are much steeper than those of the Unmix *dl*-PLA/PBS, the A/A_0 of the Unmix *l*-PLA/PBS at which Step 2 starts is higher than that of the Unmix *dl*-PLA/PBS. These results suggest that the interaction between *dl*-PLA and PBS monolayers is stronger than that between *l*-PLA and PBS monolayers.

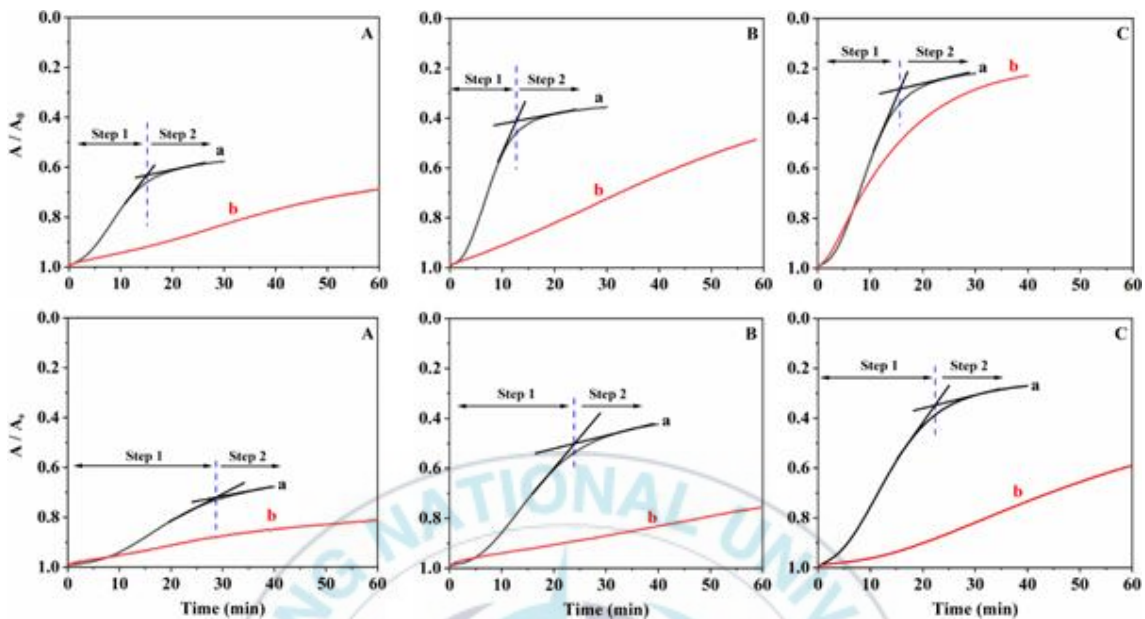


Figure 15. Area ratio vs time for *l*-PLA/PBS (Top) and *dl*-PLA/PBS (Bottom) mixture monolayers with different compositions at 4 mN/m on subphases of pH 10.7 : (A) 80/20, (B) 50/50, (C) 20/80 by mol%. Where a and b curves are from Unmix and Mix monolayers, respectively.

4.4.4. AFM Image

To compare with the bulk properties, the cast films of the mixture were prepared by spin coating. Figure 9 shows AFM images before and after alkaline hydrolysis of *l*-PLA/PBS and *dl*-PLA/PBS mixture films with 20/80 mol%, which are incompatible and compatible, respectively. Although alkaline degradation by ions occurs on the overall sample surface in both crystalline and amorphous regions, morphological changes before and after hydrolysis reflect their hydrolytic behaviors. After hydrolysis, the *dl*-PLA/PBS mixture film showed a similar morphology with partial erosion due to the slow degradation rate, while the particle-like size of the *l*-PLA/PBS mixture film clearly decreased due to the hydrolysis of surrounding particles. These results also support that the hydrolytic rate of the compatible *dl*-PLA/PBS film is slower than that of the incompatible *l*-PLA/PBS film.

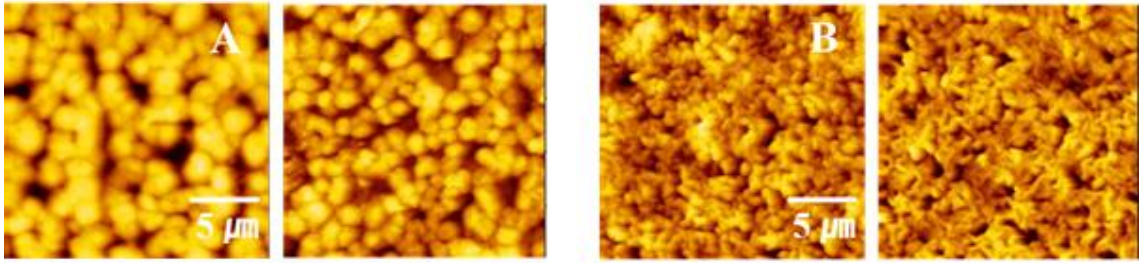


Figure 16. AFM images of *l*-PLA/PBS (A) and *dl*-PLA/PBS (B) mixture films with 20/80 by mol% before (left) and after (right) alkaline hydrolysis at pH 10.7 for 6 hr.



CHAPTER 5. Conclusions

The compatibility and hydrolytic behaviors of mixture monolayers of PLA isomers and PBS were studied by using the Langmuir system. The compatibility of a mixture monolayer was interpreted in terms of the occupied area, transition, and kinetic behavior. PBS monolayers showed an irreversibly long transition of approximately 5 mN/m and much faster alkaline hydrolysis than the other monolayers. To compare a phase-separated mixture system, a separated spreading method of each component solution was applied as a model system of a phase-separated mixture. *l*-PLA/PBS mixture monolayers with ≥ 50 mol% *l*-PLA showed good compatibility with a negative deviation in the occupied area, a change in the transition region, and a slow hydrolytic rate. In the *dl*-PLA/PBS mixture monolayers, good compatibility was observed, regardless of the mixture composition.

References

- [1] R. A. Gross, B. Kalra, Biodegradable polymers for the environment, *Science* 297 (5582) (2002) 803-807.
- [2] M. S. Reeve, S. P. McCarthy, M. J. Downey, R. A. Gross, Polylactide Stereochemistry: Effect on Enzymatic Degradability, *Macromolecules* 27 (3) (1994) 825-831.
- [3] J. M. Raquez, Y. Habibi, M. Murariu, P. Dubois, Polylactide (PLA)-based nanocomposites, *Prog. Polm. Sci.* 38 (10-11) (2013) 1504-1542.
- [4] S. Li, S. McCarthy, Influence of Crystallinity and Stereochemistry on the Enzymatic Degradation of Poly(lactide)s, *Macromolecules* 32 (13) (1999), 4454-4456.
- [5] Q. Zhou, M. Xanthos, Nanoclay and crystallinity effects on the hydrolytic degradation of polylactides, *Polym. Degrad. Stab.* 93 (8) (2008) 1450-1459.
- [6] X. Shi, J. Qin, L. Wang, L. Ren, F. Rong, D. Li, R. Wang, G. Zhang, Introduction of stereocomplex crystallites of PLA for the solid and microcellular poly(lactide)/poly(butylene adipate-co-terephthalate) blends, *RSC Adv.* 8 (22) (2018) 11850-11861.
- [7] F. R. Mayo, F. M. Lewis, Copolymerization. I. A Basis for comparing the Behavior of Monomers in Copolymerization; The

- Copolymerization of Styrene and Methyl Methacrylate, *J. Am. Chem. Soc.* 66 (9) (1944) 1594-1601.
- [8] S. Brochu, R. E. Prud'homme, I. Barakat, R. Jerome, Stereocomplexation and Morphology of Polylactides, *Macromolecules* 28 (15) (1995) 5230-5239.
- [9] Y. Deng, N. L. Thomas, Blending poly(butylene succinate) with poly(lactic acid): Ductility and phase inversion effects, *Eur. Polym. J.* 71 (2015) 534-546.
- [10] A. Bhatia, R. K. Gupta, S. Bhattacharya, H. J. Choi, Compatibility of Biodegradable Poly (lactic acid) (PLA) and Poly (butylene succinate) (PBS) Blends for Packaging Application, *KOREA-AUST RHEOL. J.* 19 (3) (2007) 125-131.
- [11] X. Hu, T. Su, P. Li, Z. Wang, Blending modification of PBS/PLA and its enzymatic degradation, *Polym. Bull.* 75(2) (2017) 533-546.
- [12] J. W. Park, S. S. Im, Phase Behavior and Morphology in Blends of Poly(L-lactic acid) and Poly(butylene succinate), *J. Appl. Polym. Sci.* 86 (3) (2002) 647-655.
- [13] R. Supthanyakul, N. Kaabbuathong, S. Chirachanchai, Random poly(butylene succinate-co-lactic acid) as a multi-functional additive for miscibility, toughness, and clarity of PLA/PBS blends, *Polymer* 105 (2016) 1-9.
- [14] L. Jompang, S. Thumsorn, J. W. On, P. Surin, C. Apawet, T. Chaichalermwong, N. Kaabbuathong, N. O-Charoen, N. Srisawat, Poly(lactic acid) and Poly(butylene succinate) Blend Fibers

- Prepared by Melt Spinning Technique, *Energy Procedia* 34 (2013) 493-499.
- [15] T. Yokohara, M. Yamaguchi, Structure and properties for biomass-based polyester blends of PLA and PBS, *Eur. Polym. J.* 44 (3) (2008) 677-685.
- [16] D. Wu, L. Yuan, E. Laredo, M. Zhang, W. Zhou, Interfacial Properties, Viscoelasticity, and Thermal Behaviors of Poly(butylene succinate)/Polylactide Blend, *Ind. Eng. Chem. Res.* 51 (5) (2012) 2290-2298.
- [17] C. Lin, L. Liu, Y. Liu, J. Leng, The compatibility of polylactic acid and polybutylene succinate blends by molecular and mesoscopic dynamics, *Int. J. Smart. Nano. Mater.* 11(1) (2020) 24-37.
- [18] J. Zhou, X. Wang, K. Hua, C. Duan, J. Ji, X. Yang, Enhanced mechanical properties and degradability of poly(butylene succinate) and poly(lactic acid) blends, *Iran. Polym. J.* 22 (4) (2013) 267-275.
- [19] S. B. Park, S. Y. Hwang, C. W. Moon, S. S. Im, Plasticizer Effect of Novel PBS Ionomer in PLA/PBS Ionomer Blend, *Macromol. Res.* 18 (5) (2010) 463-471.
- [20] P. Nugroho, H. Mitomo, F. Yoshii, T. Kume, K. Nishimura, Improvement of Processability of PCL and PBS Blend by Irradiation and its Biodegradability, *Macromol. Mater. Eng.* 286 (5) (2001) 316-323.

- [21] R. Homklin, N. Hongsriphan, Mechanical and Thermal Properties of PLA/PBS Co-continuous Blends Adding Nucleating Agent, *Energy Procedia*. 34 (2013) 871-879.
- [22] G. G. Roberts, Ed. Potential Applications of Langmuir-Blodgett Films, Langmuir-Blodgett Films, *Springer Science & Business Media*. (1990) 317-411.
- [23] W. K. Lee, J. A. Gardella, Hydrolytic Kinetic of Biodegradable Polyester Monolayers, *Langmuir* 16 (7) (2000) 3401-3406.
- [24] W. K. Lee, T. Iwata, J. A. Gardella, Hydrolytic Behavior of Enantiomeric Poly(lactide) Mixed Monolayer Films at the Air/Water Interface: Stereocomplexation Effects, *Langmuir* 21 (24) (2005) 11180-11184.
- [25] J. K. Lee, J. H. Ryou, W. K. Lee, C. Y. Park, S. B. Park, S. K. Min, Study on Hydrolytic Kinetics of Langmuir Monolayers of Biodegradable Polylactide Derivatives, *Macromol. Res.* 11 (6) (2003) 476-480.
- [26] J. K. Lee, C. S. Ha, W. K. Lee, Alkaline hydrolysis of modified poly(L-lactide) monolayers, *Mater. Sci. Eng. C.* 24 (1-2) (2004) 23-25.
- [27] N. J. Jo, T. Iwata, K. W. Lim, S. H. Jung, W. K. Lee, Degradation behaviors of polyester monolayers at the air/water interface: Alkaline and enzymatic degradations, *Polym. Degrad. Stab.* 92 (7) (2007) 1199-1203.
- [28] D. R. Lu, C. M. Xiao, S. J. Xu, Starch-based completely

- biodegradable polymer materials, *eXPRESS Polymer Letter*, 3 (6) (2009) 366-375.
- [29] M. Sheth, R. A. Kumar, V. Dave, R. A. Gross, S. P. Mccapthy, Biodegradable Polymer Blends of Poly(lactic acid) and Poly(ethylene glycol), *Applied Polymer Science*, 66 (1997) 1495-1505.
- [30] I. Armentano, M. Dottori, E. Fortunati, S. Mattioli, J. M. Kenny, Biodegradable polymer matrix nanocomposites for tissue engineering: A reivew, *Polm. Degrad. Stab.*, 95 (2010) 2126-2146.
- [31] Y. Zhong, P. Godwin, Y. Jin, H. Xiao, Biodegradable polymers and green-based antimicrobial packaging materials: A mini-review, *Advanced Industrial and Engineering Polymer Research*, 3 (2020) 27-35.
- [32] J. M. Raquez, Y. Habibi, M. Murariu, P. Dubois, Polylactide (PLA)-based nanocomposites, *Progress in Polymer Science*, 38 (2013) 1504-1542.
- [33] M. S. Reeve, S. P. McCarthy, M. J. Downey, R. A. Gross, Polylactide Stereochemistry: Effect on Enzymatic Degradability, *Macromolecules*, 27 (1994) 825-831.
- [34] K. M. Nampoothiri, N. R. Nair, R. P. John, An overview of the recent developments in polylactide (PLA) research, *Bioresource Technology*, 101 (2010) 8493-8501.
- [35] E. T. H. Vink, K. R. Rabago, D. A. Glassner, P. R. Gruber, Applications of life cycle assessment to NatureWorks™

- Poly lactide (PLA) production, *Polym. Degrad. Stab.*, 80 (2003) 403-419.
- [36] A. P. Gupta, V. Kumar, New emerging trends in synthetic biodegradable polymers - Polylactide: A critique, *Eur. Polym. J.* 43 (2007) 4053-4074.
- [37] D. Plackett, T. L. Andersen, W. B. Pedersen, L. Nielsen, Biodegradable composites based on L-poly lactide and jute fibres, *Composites Science and Technology* 63 (2003) 1287-1296.
- [38] J. Y. Moon, M. H. Kim, Y. T. Lee, H. H. Lee, Y. H. Rho, Study on the Biodegradable ability of Biodegradable Plastics PLA(Poly lactic acid) by composting, *J. Korea. Acad. Industr. Coop. Soc.*, 17 (4) (2016) 596-605.
- [39] H. Y. Lee, Control of Degradation of Poly(lactide)s by Chemical and Physical Modifications, Thesis for the Degree of Master of Engineering, Pukyong National University, Korea (2016).
- [40] Y. K. Cho, Study on synthesis of UV-curable Polyurethane Acrylates Containing Fluorine and Properties of their Composites, Thesis for the Degree of Master of Engineering, Pukyong National University, Korea (2015).
- [41] N. Jacquel, F. Freyermouth, F. Fenouillot, A. Rousseau, J. P. Pascault, P. Fuertes, R. S. Loup, Synthesis and properties of poly (butylene succinate): Efficiency of different transesterification catalysts, *J. Polym. Sci., Part A: Polym. Chem.* 49 (24) (2011) 5301-5312.

- [42] S. Mizuno, T. Maeda, C. Kanemura, A. Hotta, Biodegradability, reprocessability, and mechanical properties of polybutylene succinate (PBS) photografted by hydrophilic or hydrophobic membranes, *Polm. Degrad. Stab.*, 117 (2015) 58-65.
- [43] F. B. Ali, R. Mohan, Thermal, Mechanical, and Rheological Properties of Biodegradable Polybutylene Succinate/Carbon Nanotubes Nanocomposites, *Polym. compos.*, 31 (2010) 1309-1314.
- [44] S. W. Park, J. H. Bae, Weatherability of biodegradable polybutylene succinate (PBS) monofilaments, *J. Kor. Soc. Fish. Tech.*, 44 (4) (2008) 265-272.



Acknowledgement

Since I entered Pukyong National University in 2013, I think I have experienced and learned various things for 6 years includes my graduate school. First of all, I would like to express my deepest gratitude to my advisor, Prof. Won-Ki Lee for the continuous support of my study and research, for his patience, motivation, enthusiasm, and immense knowledge.

Prof. Won-Ki Lee gave me a chance to study and research many types of projects including biodegradable polymers. Thanks to the professor's teaching and his immense knowledge, I was able to build specialized knowledge of polymers and learn about the basic attitude of social life. I was able to grow as I am now, and sincerely thanks for always giving me advice like my father and not reluctant to say bitterly. I will try to move on to the right path by engraving the teachings of the professor while living my life in the future. I could not have imagined having a better advisor and mentor for my master's study.

And I would like to give my gratitude to my fellow lab members: especially, Seungjae Lee, my best friend, and brother. You have always supported me and helped me to do things I couldn't do. Also, you are another teacher who has guided me even before I started my master's degree. I was so happy that I had known you for 8

years and be with me forever as a good friend. Thank you so much, Seungjae.

Vishal Gavande, my first foreign friend in my life! Over the past three years, I have learned a lot about your positive mind and your endless development potential. Thank you for playing the same role as a senior and good friend for a whole life. Also, congratulations on your upcoming marriage - I hope you're always happy. Even if you finish your doctoral course well and go back to India, let's always stay in touch, bro.

Gayeon Kim, Byeonguk Kim, I hope you study hard and finish the rest semesters successfully. If you work hard, you can achieve anything.

Yong-Kwang Cho, Hakyong Lee, Youngwoo Kim, Seong-Guk Bae, GeonHo Noh, I would like to express my gratitude to the lab seniors who have always helped me. Thank you for always caring for your juniors and for giving sincere advice.

Also, I would like to thank all of the professors in the department of polymer engineering, Prof. Chan Young Park, Prof. Sang Bo Park, Prof. Bong Lee, Prof. Joo Hyun Kim, Prof. Seong Il Yoo, Prof. Mun Ho Kim, and Prof. Young Ho Eom for enlightening me the various polymeric backgrounds. Thank you, professor.

Lastly, I have to extend my thanks to my all family members who always believe and supports me. Without their support, I do not think that I could overcome the difficulties during these years. In the future, I will try to become a best son who works hard for the happiness of family.

2020. 12. 31.

Busan, Republic of Korea

Donghyeok Im

